Cellulose (2013) 20:439–452
DOI 10.1007/s10570-012-9836-8

ORIGINAL PAPER

Thermomechanical and crystallization behavior of polylactide-based flax fiber biocomposites

Andrea Arias · Marie-Claude Heuzey · Michel A. Huneault

Received: 12 September 2012 / Accepted: 22 November 2012 / Published online: 2 December 2012

Abstract In this work, the rheological, thermal and mechanical properties of melt-compounded flax fiber-reinforced polylactide composites were investigated. The effect of compounding on fiber length and diameter, and the relationship between fiber content and the crystallization behavior of the biocomposites, at various temperatures, were also examined. After melt-compounding, fiber bundles initially present were, to a large extent, broken into individual fibers and the fiber length was decreased by 75 %, while the aspect ratio was decreased by nearly 50 %. The crystallization half-time was found to decrease with increasing flax fiber content, and showed a minimum value at 105 °C for all systems. The elastic modulus was increased by 50 % in the presence of 20 wt% flax fibers. The addition of maleic anhydride-grafted polylactide had a positive effect on the mechanical properties of the biocomposite. This system is particularly interesting in the context of sustainable development as it is entirely based on renewable resources and biodegradable.

A. Arias · M.-C. Heuzey (✉)
Chemical Engineering, Center for Applied Research on Polymers and Composites—CREPEC, École Polytechnique de Montréal, Montréal, QC, Canada
e-mail: mcheuzey@polymtl.ca

M. A. Huneault
Chemical and Biotechnological Engineering Department, Université de Sherbrooke, Sherbrooke, QC, Canada

Keywords Polylactide · Flax fiber · Biocomposite · Crystallization · Mechanical properties

Introduction

The quest for materials with a reduced environmental impact motivates the development of new biodegradable composites that can represent alternatives to traditional polymer composites materials, which mostly consist of glass fibers and petrochemical-based polymers. Therefore, the manufacturing techniques, recycling and final disposal of biocomposites need to be developed or improved. Using natural fibers as reinforcement for polymeric materials has been a subject of rising interest over the last decade. Natural fibers present many advantages, including biodegradability, renewability and comparable specific mechanical properties to synthetic fibers. Composites based on natural fibers can achieve a weight reduction, leading to lower energy requirements during processing and lower costs in the final application. Availability of natural fibers for the composite industry is an important challenge; currently the markets for natural fibers are mostly concentrated in textile and food applications (Pandey et al. 2010). Flax fiber is one of the most widely used fibers in Europe and North-America; it presents a specific elastic modulus between 20 and 50 (m^2/s^2) and its specific tensile strength ranges from 250 to 1,000 (m^2/s^2) (Bismarck et al. 2005).

Working with natural fibers involves several challenges. The high hydrophilicity of natural fibers leads to poor compatibility with the commonly hydrophopic synthetic polymers. This, in turn, generally results in poor fiber wetting, poor dispersion, i.e. the presence of bundles and fiber agglomerates, and in weak fiber-matrix adhesion. In addition, it promotes water uptake by the extruded or injection-molded end-products (John and Anandjiwala 2008). Different interfacial modification routes have been investigated to increase hydrophobicity and improve interfacial properties. Chemical modification of the fiber surface involves the grafting of molecules presenting functional groups compatibles with the matrix (Li et al. 2007; Belgacem and Gandini 2008). Another possible route is to modify the matrix properties by the use of surfactants or of polymeric compatibilizer such as maleic anhydride-grafted polymers (Bondeson and Oksman 2007; Avella et al. 2008). In addition to the fiber-matrix interfacial challenge, natural fibers present particular characteristics compared to conventional fibers. For example, the fiber diameter distribution is much wider and the surface roughness is sensitive to the fiber preparation technique.

Polylactide (PLA) is a biodegradable thermoplastic polymer, which can be produced from renewable resources. Polylactide with high molecular weight for commercial applications is produced by ring-opening polymerization of lactide, a dimer of lactic acid. The stereochemical structure of PLA can be modified to yield amorphous or semicrystalline polymers depending on the L or D-isomer content used in the polymerization. However, PLA commercial grades are usually synthesized based on L-lactide with small contents of D-lactide (Garlotta 2001; Auras et al. 2004).

The mechanical and thermal properties of PLA are strongly related to crystallinity. Its thermal resistance is limited by its low glass transition, around 60 °C, unless it contains a certain level of crystallinity (Xiao et al. 2010). Fully crystallized poly L-lactide (PLLA) samples showed higher tensile modulus and strength than amorphous samples. At equal molecular weight, the tensile modulus and impact resistance increased by 20 and 100 %, respectively (Perego et al. 1996). In terms of heat deflection temperature (HDT), the value reported for crystallized PLLA was 30 °C higher than that of amorphous PLA (Harris and Lee 2008). However, PLA crystallization is typically very slow. For example, a semicrystalline commercial grade containing 2 % D-lactide presented a crystallization half-time of approximately 40 min (Li and Huneault 2007). For several applications, increasing the rate of crystallization is desired. Adding mineral nucleating agents such as talc and clay, or organic nucleants like poly(D-lactide) and more recently *N*,*N*-ethylenebis-(12-hydroxystearamide) (EBHSA) and bio-based orotic acid (Nam et al. 2006; Qiu and Li 2011) is considered as a viable route to improve the crystallization kinetics and decrease the time to achieve PLA crystallization.

The growth of PLA spherulites has been thoroughly studied using optical microscopy. The maximum spherulite growth rate has been observed between 105 and 125 °C, depending on the D-lactide content, molecular weight and processing conditions (Nam et al. 2003; Di Lorenzo 2005; Tsujia et al. 2005; Yuryev et al. 2008). In the presence of fibers, spherulitic growth can be accompanied by the growth of a transcrystalline layer on the surface of fibers. This has been shown in polypropylene (PP) composites for synthetic fibers such as Kevlar, PET, PTFE and carbon fibers (Wang and Liu 1999). The origin of transcrystallinity is not clear but several phenomena can nucleate crystallization on the surface of fibers. These include epitaxial growth based on similar crystalline lattice sizes, preferential adsorption of the polymer on the fiber surface or thermally-induced polymer orientation due to mismatch in thermal expansion between the fiber and matrix material (Wang and Liu 1999).

Wood fibers, microcrystalline cellulose and cellulose fibers have been shown to increase the crystallization temperature of PLA upon cooling (Mathew et al. 2006). This is indicative of a nucleating ability. Among these wood-based additives, wood fibers were found to have the strongest effect in terms of crystallization temperature shift. A transcrystalline layer over the wood fibers was clearly shown while little or no transcristallinity occurred on the surface of microcrystalline cellulose or on the cellulose fibers (Mathew et al. 2006).

The effect of flax fibers and their surface treatment on the crystalline development in PLA composites has also been investigated (Shanks et al. 2006). It was found that the presence of the flax fibers did not modify the crystallization temperature (T_c) significantly (less than 5 °C). The T_c changes were not sensitive to the type of surface treatment. Optical micrographs did not provide clear evidence of transcrystallinity either.

The effect of flax fibers on the crystalline development in PP has also been investigated. It was possible to grow important transcrystalline layers on the surface of flax fibers. Transcrystallinity is an important feature in composites because it can improve stress-transfer between the matrix and the fiber (Zafeiropoulos et al. 2001). Zafeiropoulos suggested that surface roughness plays a decisive role in the growth of the transcrystalline layer. Unmodified flax fibers developed a non-homogeneous layer; whereas stearic acid treated flax fibers presented a thinner but homogeneous transcrystalline layer. However, in another study on silane-modified fibers and using maleated polypropylene, transcrystallinity development was found only for untreated fibers (Biagiotti et al. 2004).

Mechanical performance of PP- and PLA-natural fiber composites has been widely investigated (Shibata et al. 2003; Arbelaiz et al. 2005; Bengtsson et al. 2007; Bledzkiet al. 2007). Properties of composites were found to depend on fiber characteristics, fiber orientation, fiber-matrix interface and matrix crystallinity. The most relevant fiber characteristics include their aspect ratio, their tensile properties and their thermal stability (Mathew et al. 2005; Bledzki et al. 2007). It is noteworthy that the reported composite properties were highly variable from one study to another. At 30 wt% of flax fibers, the elastic modulus of PLA-based composites has been shown to range from 6.8 to 9.0 GPa (as opposed to ~3 GPa for neat PLA) (Oksman et al. 2003; Bax and Mussig 2008; Le Duigou et al. 2008). Also at 30 wt% of flax fibers, the tensile strength showed an increase of about 10 % as compared to neat PLA, whose strength is of the order of 50 MPa. However some studies reported a slight reduction of this property, usually explained by the poor stress transfer across the interface, which means that there is practically no interfacial bonding between the reinforcing fiber and the polymer matrix (Oksman et al. 2003; Bodros et al. 2007; Bax and Mussig 2008). PLA elongation at break was also shown to decrease with the addition of natural reinforcements such as flax fibers and microcrystalline cellulose (MCC) (Mathew et al. 2005; Le Duigou et al. 2008). Several authors agree on the idea that any fiber can act as a weak point for fracture initiation. The elongation at break of flax fiber composites remained close to the elongation at break of the fiber (~3 %) (Baley 2002), regardless of the reinforcement content added to the system, hence making PLA slightly more brittle (typically ~6 % for neat PLA).

The aim of this work is to investigate the effect of processing and compatibilization on the properties of flax-fiber reinforced PLA biocomposites. This system is entirely based on renewable resources and is fully biodegradable; hence it represents a "green" alternative to traditional thermoplastic polymer composites. The addition of maleic anhydride-grafted PLA (PLA-g-MA) is intended to improve the fiber-matrix interaction. The crystallization behavior in quiescent isothermal and non-isothermal conditions of PLA-based biocomposites, prepared with low to moderate weight fractions of flax fibers, is investigated. Thermal, rheological and mechanical properties of the uncompatibilized and compatibilized PLA-flax fiber systems are also examined.

Experimental

Materials

The polylactide (PLA) used in this work was obtained from NatureWorks LCC. It is a semi-crystalline grade (PLA 4032D) comprising around 2 % D-lactide. Flax fibers, cut to a nominal length of 1 mm, were kindly supplied by LIMATB (France). Maleic anhydride-grafted polylactide (PLA-g-MA) was prepared in a twin-screw extruder using 2 wt% maleic anhydride and 0.25 wt% of a peroxide initiator, following a procedure reported earlier (Li and Huneault 2007). The extent of maleation of the PLA-g-MA sample was quantified by a titration method (Nabar et al. 2005; Hwang et al. 2012). The content of MA was found to be 0.8 wt%.

Samples preparation

PLA-flax fiber composites were prepared by melt mixing in an internal mixer (C.W. Brabender Plasticorder) under a nitrogen atmosphere. For all composites, the mixing time was performed for 7 min at 60 rpm and 180 °C. The nominal flax fiber content was set at 1, 5, 10 and 20 wt%. The PLA-g-MA content used was 20 wt%. Two different batches of each blend (25 g) were prepared to verify reproducibility. PLA pellets and flax fibers were previously dried at 80 °C for 24 h under vacuum. For comparison purposes, neat PLA was also processed using the same thermo-mechanical cycle and will be referred to as "compounded PLA".

As-received and compounded PLA, as well as PLA-based biocomposites, were compression molded in a

heated press from Carver Laboratory at 180 °C for about 10 min under a nitrogen atmosphere. Pressure was increased slowly from 0 to ~14 MPa. After compression molding, the samples were quenched using a water cooled press and stored in a dessicator before subsequent testing. The preparation method was chosen in order to obtain an isotropic distribution of the flax fibers in the PLA matrix and to rule out orientation effects.

Characterization techniques

Microscopy

As-received flax fibers and 60 μm thick PLA-based biocomposite films containing 5 wt% of flax fibers were observed using a Zeiss Axioskop 40 optical microscope in transmission mode. The size and state of dispersion of flax fiber before and after blending were evaluated. Diameter and length averages were calculated based on 110 fibers for dry fibers, and 210 fibers in PLA composite films.

Thermogravimetry (TGA)

Thermogravimetric analyses were performed using a TGA Q500 from TA Instruments. The measurements were carried out at a heating rate of 10 °C/min in an air atmosphere with a flow rate of 60 mL/min. Temperature ranged from 30 to 700 °C. The sample's weight was approximately 15 mg.

Rheological characterization

The rheological properties of PLA (as-received pellets and compounded) and PLA-based biocomposites with flax fiber contents of 1, 5 and 10 wt%, were evaluated at 180 °C using a stress-controlled Gemini rheometer (Malvern Instruments) and a 25 mm parallel-plate flow geometry. Measurements were performed in oscillatory mode in the linear viscoelastic region. Dynamic properties were monitored as functions of time to examine the thermal stability and behaviour of the samples. A thermal soak time of 4 min was used prior to the oscillatory measurements. Time sweep tests were carried out a frequency of 6.28 rad/s for 10 min. Frequency sweeps were performed in the linear viscoelastic regime, from low to high and high to low frequencies ranging from 0.1 to 100 rad/s, over an overall duration of 12 min.

Differential scanning calorimetry (DSC)

The thermal characteristics of PLA and PLA-based composites were examined using differential scanning calorimetry (DSC Q1000 from TA Instruments) under a helium atmosphere. A sample size of approximately 10 mg was used. Before all DSC tests, the thermal history was removed by heating the samples from 30 to 200 °C and maintaining at 200 °C for 3 min. The non-isothermal characterization was carried out by cooling the samples from 200 down to 30 °C using cooling rates of 2, 5 and 10 °C/min and then re-heating from 30 to 200 °C at a heating rate of 10 °C/min.

In the case of the isothermal tests, samples were cooled from 200 °C to different crystallization temperatures T_c: 90, 100, 105, 110, and 120 °C, at a rate of 50 °C/min. The samples were then maintained at this temperature until the crystallization was completed. Finally, the samples were heated back from the crystallization temperature to 200 °C at a heating rate of 20 °C/min to measure the melting enthalpy.

Mechanical characterization

Tensile testing was performed according to ASTM D638 for tensile properties of plastics using an Instron universal testing machine. Measurements were carried out using standard type V dog-bone shaped samples with a crosshead speed of 1 mm/min, and using a load cell of 5 kN. Six specimens were tested for each formulation.

Dynamic mechanical thermal analysis (DMTA)

Dynamic mechanical thermal analysis was performed in a dual cantilever bending mode by using a DMA 2980 from TA Instruments. The measurements were conducted at 1 Hz at a heating rate of 2 °C/min from room temperature to 130 °C. The test specimens were 2 mm thick, 35 mm long and 12 mm wide.

Results and discussion

Thermal stability of fibers

The thermal stability of the flax fibers was evaluated using the TGA technique. Figure 1 shows the relative weight drop (left ordinate) and the weight drop first derivative (right ordinate) as functions of temperature

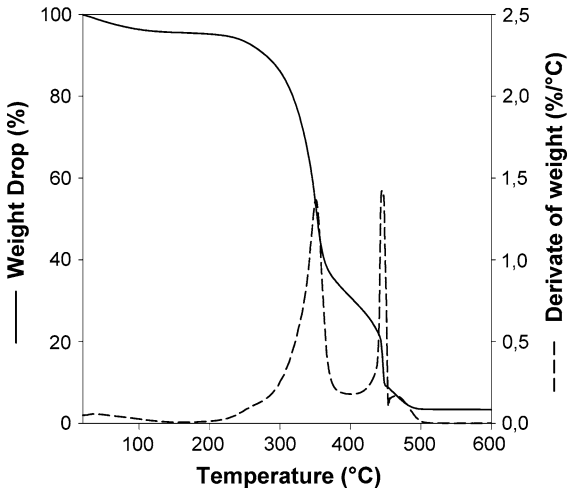

Fig. 1 Thermogravimetry results for flax fibers

in air. Three different rapid weight loss regions can be identified. A first one, accounting for about 5 % weight loss occurs between room temperature and about 100 °C. This weight loss can be associated to residual moisture loss. The second important weight loss, accounting for more than 50 % of the total loss, takes place between 220 and 380 °C. This weight loss region is in the degradation interval of the flax fibers and is most commonly associated to the first steps of hemicelluloses and cellulose depolymerization. A third region can be distinguished from the second one when observing the first derivative peaks. The third weight loss region, above 400 °C, accounts for the final 40 % weight loss. This weight loss can be associated to the final stages of degradation of cellulose and hemicelluloses. Flax fibers present a complex chemical structure based on crystalline and amorphous cellulose regions contained into a lignin-hemicellulose matrix (Bismarck et al. 2005). During thermal degradation, several parallel reactions take place. Thermal decomposition starts with hemicelluloses, closely followed by lignin and subsequently by cellulose (George et al. 2001). It has been pointed out that in an inert atmosphere, hemicellulose degrades preferentially from 200 to 325 °C, lignin from 280 to 400 °C and cellulose from 300 to 400 °C (Ramiah 1970; Shafizadeh and Bradbury 1979). These intervals can shift in the presence of oxygen. Consequently, the second peak in Fig. 1 represents the superposition of three depolymerization reactions. Several authors have indicated that the third peak corresponds to the further degradation of residues and aromatic substances (Van de Velde and Baetens 2001; Le Troedec et al. 2008). Considering these results, the flax fibers should withstand compounding with the PLA matrix at 180 °C under a nitrogen atmosphere.

Fiber morphology

Since fiber attrition and breakup during processing is a major concern, it is important to verify the fiber dimensions and aspect ratio after compounding. Figure 2 shows the optical micrographs of as-received flax fibers (2a, b) and a PLA-biocomposite film with 5 wt% of flax fibers (2c, d). The as-received flax fibers are in the form of bundles and single fibers, with an approximate length of 1 mm (the original nominal length). In comparison, the flax fibers in the composite show less fiber bundles and more single flax fibers, with length below 300 μm (Fig. 2c, d).

Figure 3 presents the length, diameter and aspect ratio distributions of the flax fibers before and after compounding. The length distribution of the as-received flax fibers (Fig. 3a) varied from 875 to 1,275 μm, with a weighted mean length of 1,015 μm. More than 80 % of fibers were found between 975 and 1,075 μm in length. After compounding, the distribution of fiber length varied from 75 to 475 μm, and the weighted mean length decreased by about 75 %, reaching 250 μm. The fiber diameter, shown in Fig. 3b, exhibited a bimodal distribution before compounding. The first mode around 30 μm probably represents the single fiber population in the sample, which accounts for ~60 % of fibers. The remaining ~40 % of fibers had a mode centered on 110 μm that is associated to the bundle population. After compounding, the diameter presented a narrow unimodal distribution, where more than 95 % of the fiber diameters were below 40 μm and the presence of bundles was negligible. The aspect ratio of the as-received flax fibers before compounding (Fig. 3c) showed a wide distribution. Its value varied from 4 to 76, and it presented a weighted mean around 28. After compounding, the aspect ratio distribution became narrower so that 70 % of the compounded flax fibers exhibited an aspect ratio between 10 and 20. Because the length, diameter and aspect ratio decreased during compounding, it was clear that breakup occurred simultaneously in the longitudinal and transverse

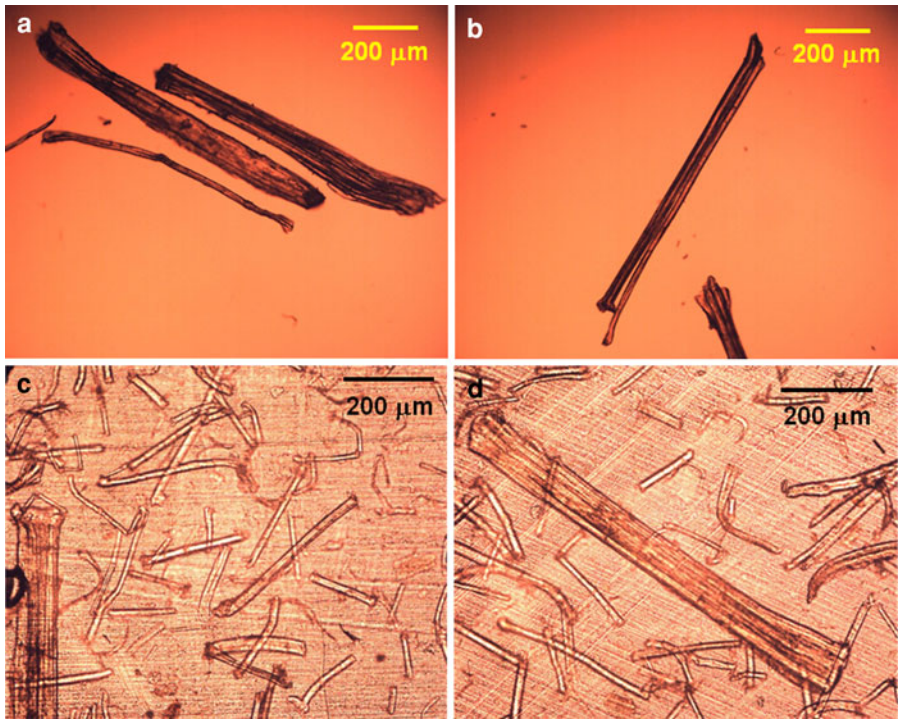

Fig. 2 Optical micrographs of: **a**, **b** as-received flax fibers and **c**, **d** 5 wt% PLA-flax fiber composite film, 60 μm thick

directions. However, a more homogeneous distribution was observed in the cases of diameter and aspect ratio after compounding. Flax fiber attrition has been reported earlier in PLA (Oksman et al. 2009) and polypropylene composites (Barkoula et al. 2010). In PLA, flax fiber length was shown to decrease from ~5 to 1 mm after twin screw extrusion. Similar effects have been reported for cellulose nanocomposites; mean length of ramie whiskers has shown a decrease of 50 % after extrusion film process (Alloin et al. 2011).

Rheology

It is well known that the presence of water and high temperature lead to the random scission of PLA chains, decreasing molecular weight and thus viscosity (Madhavan Nampoothiri et al. 2010). Considering that flax fibers are hydrophilic, it is difficult to completely eliminate their water content. This residual water can have an impact on the hydrolytic chain scission of PLA. Since molecular weight and viscosity are intimately linked, rheological measurements were used as a mean to investigate PLA thermal degradation at processing temperature. Figure 4 presents the complex viscosity at 180 °C as a function of time, for as-received and compounded PLA and various PLA-flax fiber based composites. The viscosity of the compounded PLA was initially around 3,000 Pa.s. It was relatively stable up to 200 s and then dropped slightly, loosing around 5 % of its value after 600 s. A similar test was carried out on the as-received PLA. The initial viscosity of the pellets was around 4,400 Pa.s, but its drop was slightly more important than for compounded PLA, it decreased ~2 % per minute, reaching 3,600 Pa.s after 600 s. The difference between the as-received and compounded PLA viscosity can be associated to chain scission during compounding, and also in a potential plasticization of the PLA by low molecular weight degradation products such as lactic acid or lactic acid oligomers. These low molecular weight products are known to efficiently plasticize PLA (Martin and Averous 2001).

Figure 4 also shows that the complex viscosity increased with fiber content. At 10 wt% of flax fibers, the initial viscosity of the composite was close to 4,500 Pa.s, which somewhat exceeds the as-received PLA viscosity. It also represents a 50 % increase in comparison with compounded PLA. However the composite's viscosity showed a slightly more important

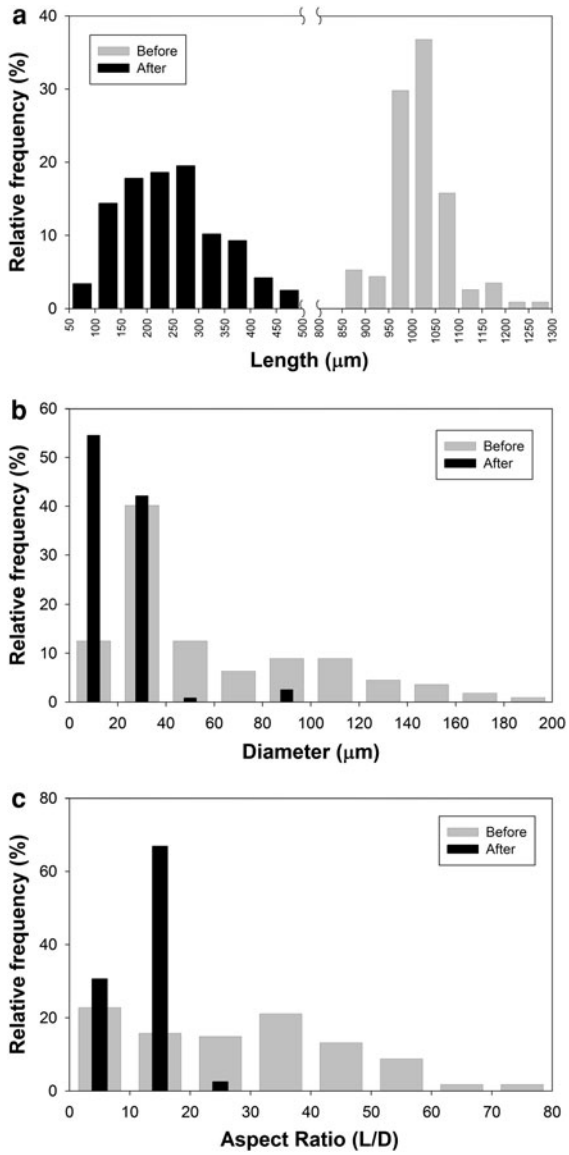

Fig. 3 Distribution of flax fiber dimensions before and after compounding: **a** length, **b** diameter, and **c** aspect ratio

drop with time. On average, the complex viscosity of compounded PLA, as well as 1 and 5 wt% flax fiber composites, dropped by ~1 % per minute. This value increased to around 2 % per minute for the PLA-10 wt% flax fiber composite. It is noteworthy, however, that the residence time in most polymer processing operations is much shorter than the time sweeps in this investigation (14 min, including thermal soak time) or than the laboratory mixing/molding time (7 min mixing and 10 min compression molding). Molecular weight loss during compounding in industrial

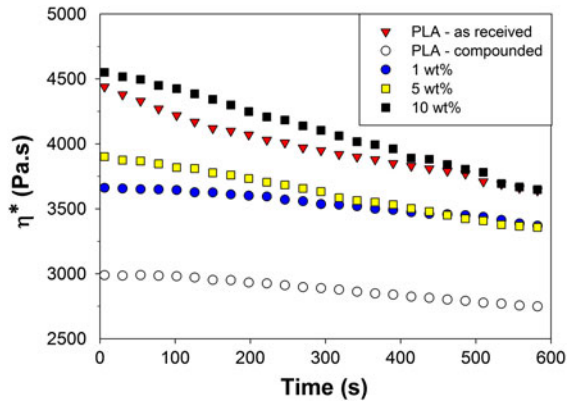

Fig. 4 Time sweep at 180 °C for as-received and compounded PLA and PLA-based flax fiber composites with various fiber contents

conditions may therefore be smaller than the effect found in this investigation, depending on the specific thermomechanical history. Considering that the PLA viscosity is a function of molecular weight to the power 3.4 (Palade et al. 2001), the viscosity drop between the as-received and the compounded PLA can be associated with a 8 % drop in average molecular weight over 10 min. In the high molecular weight range, the mechanical properties of polymers are not expected to differ significantly for such a change in average molecular weight (Perego et al. 1996).

Figure 5 shows the complex viscosity of PLA and PLA-based composites as a function of frequency at 180 °C. As-received and compounded PLA presented a shear-thinning behaviour characterized by a plateau

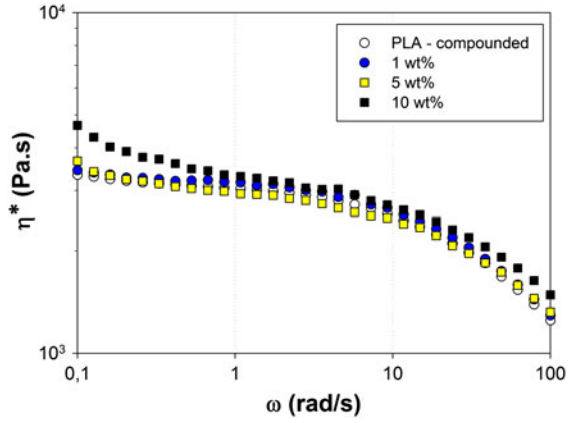

Fig. 5 Complex viscosity at 180 °C for PLA-based composites and compounded-PLA

viscosity at low frequency, followed by a power-law decrease as frequency increases. PLA-based composites also exhibited non-Newtonian behaviour. At low frequency, viscosity increased slightly as flax fiber content increased; composite at 10 wt% exhibited a complex viscosity close to 5,000 Pa.s at 0.1 rad/s, and there is no indication of a plateau in this frequency range. This phenomenon may be associated with the formation of a fiber network; however, this hypothesis requires further investigation.

Crystallization

Isothermal crystallization tests were carried out between 90 and 120 °C. The relative degree of crystallinity as function of time is shown in Figs. 6 and 7 for compounded PLA and PLA-based composites, respectively. Figure 6 compares the relative degree of crystallinity of compounded PLA for different crystallization temperatures. Isothermal crystallization of as-received PLA pellets at 105 °C is also shown for comparison. All curves have the expected sigmoidal shape. The PLA-compounded samples at 100, 105 and 110 °C showed very similar behaviour and exhibited a faster crystallization than the samples crystallized at 90 and 120 °C. In terms of crystallization half-time, $t_{1/2}$, defined as the time required to reach half of the final crystallinity, the compounding step leads to a $t_{1/2}$ drop from $\sim$40 to $\sim$4 min at 105 °C. One potential reason that could explain such a boost in crystallization rate may come from the decrease in polymer viscosity described in the previous section. The general increase in polymer chain mobility, either by a general average molecular weight reduction during compounding or to a plasticization effect coming from low molecular weight degradation products may considerably speed up the crystalline growth rate.

Figure 7 examines the effect of the fiber content on the relative degree of crystallinity at 90 °C for PLA-based composites. These samples exhibited a similar induction period of 3–4 min prior to a significant crystallinity growth. However, the subsequent crystalline development was clearly accelerated as the flax fiber content was increased. The crystallization half-time, $t_{1/2}$, decreased from 10.5 min for compounded PLA to 7 min for the 10 wt% flax fiber composite at 90 °C. This indicates that the flax fiber may play a nucleating role in the PLA crystallization. A similar behavior was observed in the overall temperature range investigated.

The isothermal crystallization kinetics of polymers during the crystalline growth rate stage (i.e. after induction and prior to secondary crystallization) is often described by the classical Avrami equation (Avrami 1939):

$$X_c(t) = 1 - \exp(-Kt^n)$$

where X_c is the relative degree of crystallinity, K is a rate constant and n is the Avrami exponent that depends on the nature of nucleation and growth geometry of the crystals. Its value is typically between 2 and 4 for polymer crystallization.

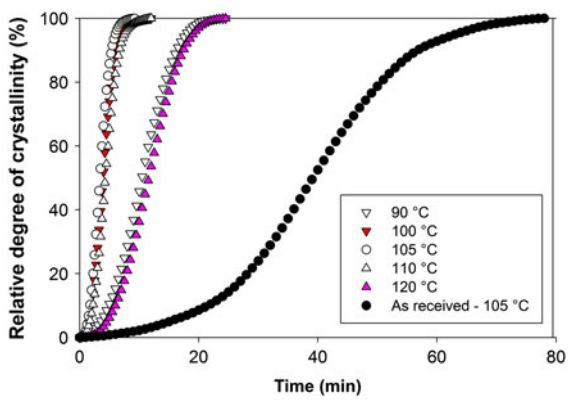

Fig. 6 Relative degree of crystallinity as function of crystallization time for compounded PLA at different temperatures, and as-received PLA at 105 °C

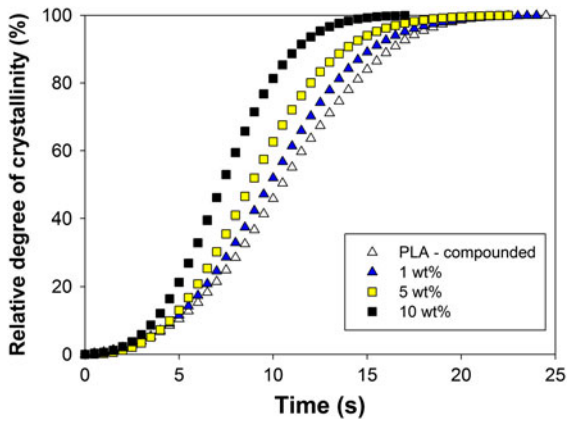

Fig. 7 Relative degree of crystallinity as function of crystallization time at 90 °C for PLA-based composites and compounded PLA

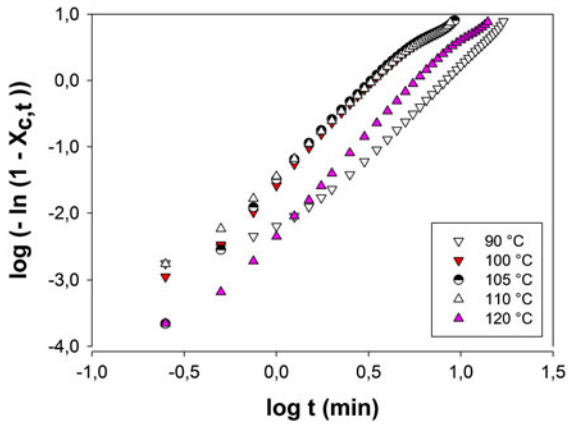

Fig. 8 Avrami plots for the PLA–10 wt% flax fiber composite at various crystallization temperatures

Figure 8 presents log $(-\ln(1 - X_c(t)))$ against log t. This representation enables graphical evaluation of K and n from the graph ordinate and slope, respectively. For each composite, a series of straight lines were obtained showing that the crystallization kinetics followed a classical Avrami relationship. The values of n and K were obtained from the linear graph portion and are summarized in Table 1.

The average value of n is about 2.7 for compounded PLA, and 1.9 for as-received PLA. This significant difference is intriguing and could indicate different nucleation and growth mechanisms. Further investigation will be required to clarify this point. The average Avrami exponents obtained for the composites are 2.9, 2.8 and 2.8 for 1, 5 and 10 wt% of flax fibers, respectively, hence very similar to the one obtained for compounded PLA. A large variety of n values can be found in the literature for PLA. Xiao et al. (2010) have reported $n = 1.9$ for neat PLA at 120 °C. They also determined similar values for PLA–triphenyl phosphate and PLA–talc composites, at temperatures ranging from 113 to 128 °C. On the other hand, larger n values have been reported for neat PLA and PLA–clay nanocomposites (from 3 to 6) (Najafi et al. 2012). It is unclear at this point why so different results can be encountered.

It has been proposed that PLA predominantly exhibit homogeneous nucleation and two-dimensional crystal growth (Xiao et al. 2010). PLA-based composites, on the other hand, will undergo mostly heterogeneous nucleation because of the presence of the fibers, with their growth dimensions being dependent on the filler geometry. Fiber-type fillers may promote an enhanced nucleation of spherulitic growth along fibers, and a columnar crystal morphology may be developed if the nucleation density is high (Wang and Liu 1999). Hence, the small difference in the Avrami exponent between compounded PLA and PLA composites may be explained by the development of two-dimensional crystal growth in both cases. Another explanation could be a low interaction between the fibers and the polymer chains; hence the geometry of the PLA crystals would not be modified much by the presence of the fibers.

The effect of crystallization temperature on crystallization half-time, $t_{1/2}$, is shown in Fig. 9. All systems presented a "u" shape with a minimum $t_{1/2}$ in

Table 1 Kinetics parameters obtained from the Avrami analysis for flax fiber-reinforced PLA

Sample	n, K (min^{-n})	T_c (°C)				
		90	100	105	110	120
PLA—as received	n	–	–	1.9	–	–
	K	–	–	3.51E−04	–	–
PLA—compounded	n	2.6	2.7	2.8	2.7	2.8
	K	1.56E−03	1.59E−02	2.03E−02	1.36E−02	6.86E−04
PLA—1 wt%	n	2.5	3.1	2.8	2.9	3.0
	K	2.17E−03	1.48E−02	1.81E−02	1.26E−02	4.96E−04
PLA—5 wt%	n	2.7	2.8	2.8	2.7	3.1
	K	2.07E−03	1.46E−02	1.63E−02	2.29E−02	1.54E−03
PLA—10 wt%	n	2.6	2.8	3.0	2.6	3.0
	K	3.97E−03	2.90E−02	2.65E−02	3.86E−02	5.20E−03

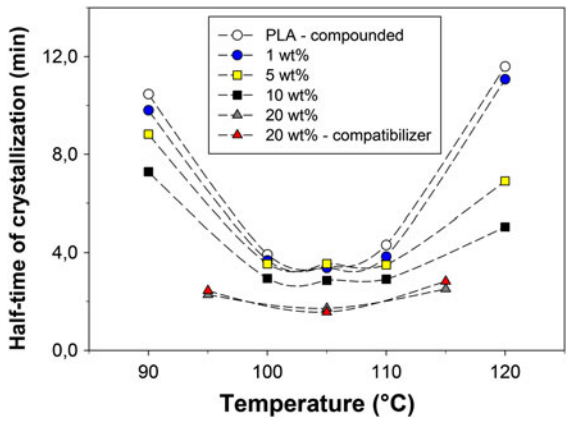

Fig. 9 Isothermal crystallization half time as function of temperature for PLA-based composites and compounded PLA

the 100–110 °C range. We can associate the "u" shape of the $t_{1/2}$ curve to two competing phenomena controlling the crystallization process: the nucleation rate and the chain mobility. The nucleation rate increases with the amount of undercooling, i.e. the difference between the melting temperature and the crystallization temperature. By contrast, the chain mobility is enhanced as the temperature increases. For the as-received PLA, the minimum half-time was around 39 min at 105 °C (not shown). The minimum half-time for compounded PLA and for 1 and 5 wt% flax fiber composites was significantly reduced, to around 3.5–4 min at the same temperature. With 10 and 20 wt% of flax fibers, the half-time was further decreased, below 3 min. Outside the 100–110 °C optimal crystallisation temperature range, the effect of fibre content was more significant with the highest flax concentrations leading to the lowest half-times. Some authors have suggested that the decrease in the induction time of semicrystalline polymers, in the presence of both synthetic and natural fibers, is due to the fact that surface roughness plays a key role in increasing crystal nucleus density (Wang and Liu 1999; Zafeiropoulos et al. 2001; Hermida and Mega 2007). Flax fibers may contribute to both phenomena, i.e. they may act as nucleation agents and improve local chain mobility, i.e. in the vicinity of the fibers. Further evidence of flax fibers nucleating ability and effect on local chain mobility is discussed below.

Figure 10 presents the DSC non-isothermal thermograms obtained for PLA (as-received and compounded), and PLA-based composites cooled at rates

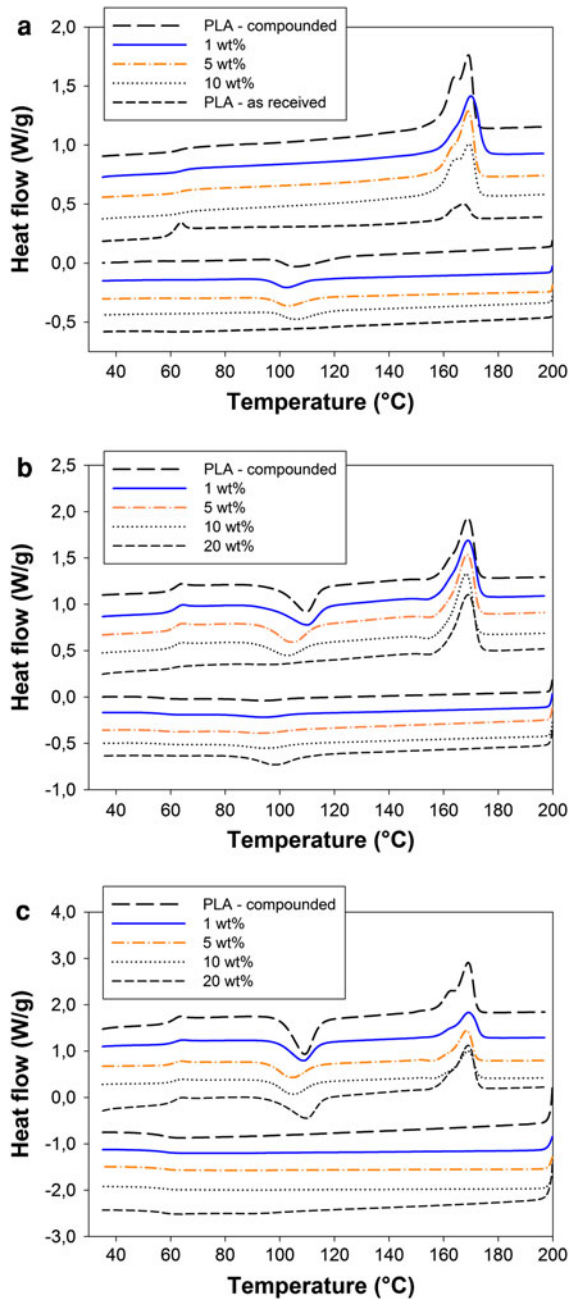

Fig. 10 DSC thermograms for PLA-based composites, compounded PLA and as-received PLA, cooling rates of: **a** 2 °C/min, **b** 5 °C/min and **c** 10 °C/min

of 2, 5 and 10 °C/min. The glass transition temperature remained nearly constant for all composites and for PLA–compounded as well. According to the DSC thermograms (Fig. 10a, b, c) the T_g values are close to 60 °C in all cases. The crystallization and melting

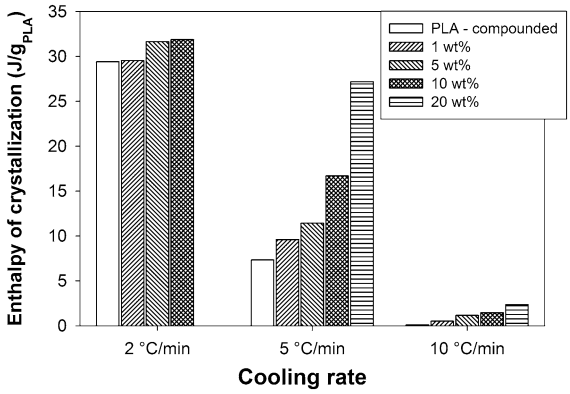

Fig. 11 Enthalpy of crystallization during cooling for PLA-based composites and compounded PLA

enthalpies obtained from the peak integration of the non-isothermal data (Fig. 10) are summarized in Fig. 11. At 2 °C/min cooling (Fig. 10a), the composites reached complete crystallization during the cooling stage, i.e. no crystallization peaks were formed upon reheating. As-received PLA did not crystallize under any cooling or heating stage. Compounded PLA exhibited a crystallization enthalpy of ~29 J/g which is equivalent to 31 % of crystallinity (using 93.7 J/g as the theoretical value for the heat of fusion of PLA crystals (Fischer et al. 1973)). The crystallinity developed upon cooling increased slightly as flax fiber content increased. At 10 wt% of fibers, the total crystallinity reached a value of 34 %. At 5 °C/min cooling (Fig. 10b), crystallization upon cooling was incomplete. It was completed via cold crystallization on the subsequent reheating cycle. Upon cooling, the crystallization enthalpy grew from ~7 to ~28 J/g for flax fiber contents from 0 to 20 wt%, respectively. Maximum content of crystals reached during the cooling and second heating varied from 34 % for compounded PLA, to 37 % for 20 wt% flax fiber composites. Upon 5 °C/min cooling, PLA reached ~20 % of its total crystallinity, while the composite at 10 wt% of flax fiber reached ~50 % of its total crystallinity; at 20 wt% of flax fiber, about 80 % of the total crystallinity was reached during the cooling stage. However, the total crystallinity achieved in all cases was between ~30 to ~37 %. The crystallization peak upon cooling was shifted to higher temperatures as the fiber concentration increased, indicating that the crystallization started earlier under non-isothermal conditions. The cold crystallization peak followed the opposite tendency; it was displaced to lower temperatures for PLA-based composites, suggesting enhanced local mobility of polymer chains. Presence of fibers in the polymer matrix could be understood as "obstacles", going against the mobility and slippage of polymers chains; however, if these so-called obstacles locally multiply the number of crystal nucleus, it will be easier for the polymer chains to reach one nucleus, reducing the displacement and enhancing the local mobility.

At 10 °C/min cooling (Fig. 10c), the crystallinity reached during cooling was negligible; only cold crystallization process took place in all samples. The crystallinity content built during cooling represented maximum ~8 % of the total crystallinity of PLA-based composites. Total crystallinity values ranged from ~30 % for compounded PLA to ~33 % for PLA-20 wt% flax fiber composite.

If the crystallization initiates preferentially at the fiber surface, a transcrystalline morphology will be privileged, creating crystalline regions that could act as physical crosslink between matrix and filler (Mathew et al. 2006). This fact could most probably give a stronger fiber-matrix interphase, and consequently better mechanical performance. However the industrial processing of composites requires really fast cooling rates; it is still a challenge to develop PLA-based composites that crystallizes faster.

Thermo-mechanical properties

Figure 12 presents the dynamic storage modulus in dual cantilever bending mode, as a function of temperature and for compounded PLA and PLA-flax fiber composites. Maleic anhydride grafted polylactide, PLA-g-MA, was utilized as a compatibilizer in this analysis. The compounded PLA and PLA/PLA-g-MA blend showed a similar behavior: the storage modulus decreased dramatically at temperatures higher than ~70 °C, due to the softening of the composite when the glass transition temperature (T_g ~ 60 °C) is exceeded; the modulus started to increase after 100 °C recovering around 15 % of the former reduction. This behavior may be explained by the cold crystallization process simultaneously taking place during the test. In fact, the partial organization of the polymer chains due to crystallization increases the resistance of the material to thermo-mechanical

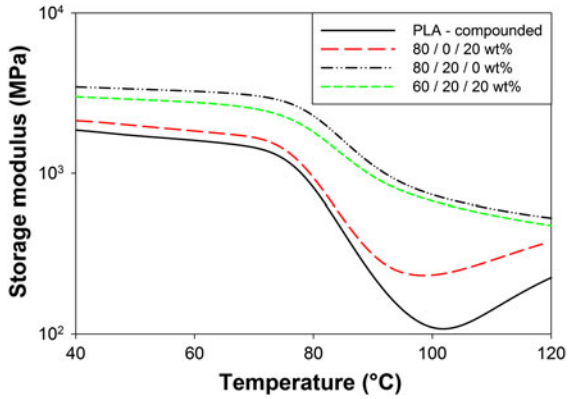

Fig. 12 DMTA results for various PLA systems. Tests were performed at 1 Hz and heating rate of 2 °C/min. The three numbers in the legend describe wt% of PLA, flax fiber and PLA-g-MA, respectively

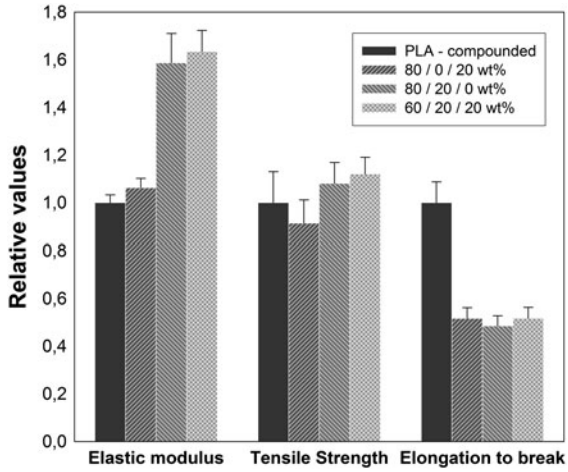

Fig. 13 Tensile properties of various PLA systems. The three numbers in the legend describes wt% of PLA, flax fiber and PLA-g-MA, respectively

stresses. Similar results have been reported by Oksman et al. (2003) for PLA-flax fiber composites.

Figure 12 shows that the presence of 20 wt% of flax fibers has doubled the storage modulus of PLA at temperatures below ~70 °C, indicating the reinforcement effect of this filler. Compounded PLA exhibited a storage modulus of ~2,200 MPa before softening; this parameter reached ~4,000 MPa at 20 wt% of fiber content. During the softening process, PLA-flax fiber composites did not exhibit a recovery phenomenon, most probably because the crystallization has been completed upon previous cooling in these samples, due to the nucleating effect of the fibers. In addition, the storage modulus reduction was much smaller than for PLA and the PLA/PLA-g-MA blend above T_g, hence the fibers helped in retaining the mechanical properties at higher temperatures. This improvement is critical since one of the main drawbacks of PLA is its poor temperature resistance.

Tensile properties

The mechanical properties of PLA-20 wt% flax fiber composites in tensile testing were characterized and compared with those of the matrix. Three different formulations were compared. Figure 13 presents the relative Young modulus, tensile strength and elongation at break of various PLA systems. The relative properties are the composite properties divided by that of the compounded matrix. Compounded PLA had a tensile strength of 53 MPa, a modulus of 3.4 GPa and an elongation at break of 6 %.

The addition of 20 wt% of flax fibers increased the Young modulus by approximately 50 %, though the use of PLA-g-MA provided a slightly larger increase. The tensile strength is directly related to the ability of the materials to transfer stress from the matrix to the reinforcing fibers (Agarwal et al. 2006). Tensile strength increased by 10 % as flax fibers were added. The combination of 20 wt% PLA-g-MA and 20 wt% flax fiber resulted in the highest tensile strength and elastic modulus for all systems. This could suggest that the PLA-g-MA improved the fiber-matrix interfacial interaction. The elongation at break, however, decreased by about 50 % for all systems, as expected from the increased rigidity. Figure 13 also shows that the tensile strength of compounded neat PLA was slightly decreased (~10 %) by the addition of the 20 wt% PLA-g-MA, possibly explained by the lower molecular weight of the PLA-g-MA.

Conclusions

The goal of this study was to prepare flax-fiber reinforced PLA biocomposites by melt compounding, and to characterize their thermomechanical and crystallization behavior. Main findings can be summarized as follow: The mean flax fiber length was decreased by 75 % from its initial length of 1 mm after

compounding. In terms of diameter, most fiber bundles were broken up during compounding, with the fiber diameter reaching about 30 μm in the biocomposites, hence slightly larger than for a single fiber. Overall the aspect ratio decreased by about two times after compounding (from ~30 to ~15), and the distribution was much narrower. Rheological characterization showed that the complex viscosity of the composites was thermally unstable, dropping by ~2 % per minute at the highest concentration of fibers (10 wt%). The isothermal crystallization half-time of the composites showed a significant decrease as flax fiber content increased. Non-isothermal crystallization also exhibited an increase in the crystallization rate of biocomposites during cooling, as the flax fiber content increased; however total crystallinity remained nearly constant, around 36 %. A significant rise in the Young modulus (~50 %) was obtained in the presence of 20 wt% flax fibers, while tensile strength remained approximately constant and a decrease of 50 % in the elongation at break was observed. Tensile properties indicate that flax fibers have a significant potential as reinforcement for the PLA matrix, however further investigation is needed to improve stress transfer from the matrix to the fiber during mechanical solicitation. The addition of PLA-g-MA to the composite also affected positively the mechanical performance. The PLA-flax fiber composite system is particularly interesting in a context of reduced environmental impact as it is entirely based on renewable resources, fully biodegradable, while exhibiting good thermomechanical properties.

Acknowledgments The authors gratefully acknowledge the Natural Sciences and Engineering Research Council of Canada (NSERC) for funding. They also thank Gilles Ausias from Laboratoire d'Ingénierie des Matériaux de Bretagne (LIMATB) for providing the flax fibers, and Cristina Kawano for her help with the optical microscopy measurements.

References

Agarwal BD, Broutman LJ et al (2006) Analysis and performance of fiber composites. Wiley, New Jersey

Alloin F, Alessandra DA et al (2011) Poly(oxyethylene) and ramie whiskers based nanocomposites: influence of processing: extrusion and casting/evaporation. Cellulose 18(4): 957–973

Arbelaiz A, Fernandez B et al (2005) Mechanical properties of flax fibre/polypropylene composites. Influence of fibre/matrix modification and glass fibre hybridization. Compos A Appl Sci Manuf 36(12):1637–1644

Auras R, Harte B et al (2004) An overview of polylactides as packaging materials. Macromol Biosci 4(9):835–864

Avella M, Bogoeva-Gaceva G et al (2008) Poly(lactic acid)-based biocomposites reinforced with kenaf fibers. J Appl Polym Sci 108(6):3542–3551

Avrami M (1939) Kinetics of phase change. I General theory. J Chem Phys 7(12):1103–1112

Baley C (2002) Analysis of the flax fibres tensile behaviour and analysis of the tensile stiffness increase. Compos A Appl Sci Manuf 33(7):939–948

Barkoula NM, Garkhail SK et al (2010) Effect of compounding and injection molding on the mechanical properties of flax fiber polypropylene composites. J Reinf Plast Compos 29(9):1366–1385

Bax B, Mussig J (2008) Impact and tensile properties of PLA/Cordenka and PLA/flax composites. Compos Sci Technol 68(7–8):1601–1607

Belgacem MN, Gandini A (2008) Surface modification of cellulose fibres. Monomers, polymers and composites from renewable resources. É. F. d. P. e. INPG pp 385–400

Bengtsson M, Baillif ML et al (2007) Extrusion and mechanical properties of highly filled cellulose fibre-polypropylene composites. Compos A Appl Sci Manuf 38(8):1922–1931

Biagiotti J, Puglia D et al (2004) A systematic investigation on the influence of the chemical treatment of natural fibers on the properties of their polymer matrix composites. Polym Compos 25(5):470–479

Bismarck A, Mishra S et al (2005) Plant fibers as reinforcement for green composites. In: Mohanty AK, Misra M, Drzal LT (eds) Natural fibers, biopolymers, and biocomposites. CRC Press Taylor & Francis Group, Boca Raton, pp 37–108

Bledzki AK, Mamun AA et al (2007) Abaca fibre reinforced PP composites and comparison with jute and flax fibre PP composites. Express Polym Lett 1(11):755–762

Bodros E, Pillin I et al (2007) Could biopolymers reinforced by randomly scattered flax fibre be used in structural applications? Compos Sci Technol 67(3–4):462–470

Bondeson D, Oksman K (2007) Dispersion and characteristics of surfactant modified cellulose whiskers nanocomposites. Compos Interfaces 14:617–630

Di Lorenzo ML (2005) Crystallization behavior of poly(L-lactic acid). Eur Polymer J 41(3):569–575

Fischer EW, Sterzel HJ et al (1973) Investigation of the structure of solution grown crystals of lactide copolymers by means of chemical reactions. Kolloid-Z Z Polym 251(11):980–990

Garlotta D (2001) A litterature review of poly(Lactic acid). J Polym Environ 9(2):63–84

George J, Klompen ETJ et al (2001) Thermal degradation of green and upgraded flax fibres. Adv Compos Lett 10(2): 81–88

Harris AM, Lee EC (2008) Improving mechanical performance of injection molded PLA by controlling crystallinity. J Appl Polym Sci 107(4):2246–2255

Hermida E, Mega V (2007) Transcrystallization kinetics at the poly(3-hydroxybutyrate-co-3-hydroxyvalerate)/hemp fibre interface. Compos A Appl Sci Manuf 38(5):1387–1394

Hwang SW, Lee SB et al (2012) Grafting of maleic anhydride on poly(L-lactic acid). Effects on physical and mechanical properties. Polym Test 31(2):333–344

John MJ, Anandjiwala RD (2008) Recent developments in chemical modification and characterization of natural fiber-reinforced composites. Polym Compos 29(2):187–207

Le Duigou A, Pillin I et al (2008) Effect of recycling on mechanical behaviour of biocompostable flax/poly(L-lactide) composites. Compos A Appl Sci Manuf 39(9): 1471–1478

Le Troedec M, Sedan D et al (2008) Influence of various chemical treatments on the composition and structure of hemp fibres. Compos A Appl Sci Manuf 39(3):514–522

Li HB, Huneault MA (2007) Effect of nucleation and plasticization on the crystallization of poly(lactic acid). Polymer 48(23):6855–6866

Li X, Tabil LG et al (2007) Chemical treatments of natural fiber for use in natural fiber-reinforced composites: a review. J Polym Environ 15(1):25–33

Madhavan Nampoothiri K, Nair NR et al (2010) An overview of the recent developments in polylactide (PLA) research. Bioresour Technol 101(22):8493–8501

Martin O, Averous L (2001) Poly(lactic acid): plasticization and properties of biodegradable multiphase systems. Polymer 42(14):6209–6219

Mathew AP, Oksman K et al (2005) Mechanical properties of biodegradable composites from poly lactic acid (PLA) and microcrystalline cellulose (MCC). J Appl Polym Sci 97(5):2014–2025

Mathew AP, Oksman K et al (2006) The effect of morphology and chemical characteristics of cellulose reinforcements on the crystallinity of polylactic acid. J Appl Polym Sci 101(1):300–310

Nabar Y, Raquez JM et al (2005) Production of starch foams by twin-screw extrusion: effect of maleated poly(butylene adipate-co-terephthalate) as a compatibilizer. Biomacromolecules 6(2):807–817

Najafi N, Heuzey MC et al (2012) Crystallization behavior and morphology of polylactide (PLA) and PLA/clay nanocomposites in the presence of chain extenders. Polym Eng Sci, Manuscript accepted for publication

Nam JY, Ray SS et al (2003) Crystallization behavior and morphology of biodegradable polylactide/layered silicate nanocomposite. Macromolecules 36(19):7126–7131

Nam JY, Okamoto M et al (2006) Morphology and crystallization kinetics in a mixture of low-molecular weight aliphatic amide and polylactide. Polymer 47(4):1340–1347

Oksman K, Skrifvars M et al (2003) Natural fibres as reinforcement in polylactic acid (PLA) composites. Compos Sci Technol 63(9):1317–1324

Oksman K, Mathew AP et al (2009) The influence of fibre microstructure on fibre breakage and mechanical properties of natural fibre reinforced polypropylene. Compos Sci Technol 69(11–12):1847–1853

Palade LI, Lehermeier HJ et al (2001) Melt rheology of high L-content poly(lactic acid). Macromolecules 34(5):1384–1390

Pandey JK, Ahn SH et al (2010) Recent advances in the application of natural fiber based composites. Macromol Mater Eng 295(11):975–989

Perego G, Cella GD et al (1996) Effect of molecular weight and crystallinity on poly(lactic acid) mechanical properties. J Appl Polym Sci 59(1):37–43

Qiu Z, Li Z (2011) Effect of orotic acid on the crystallization kinetics and morphology of biodegradable poly(L-lactide) as an efficient nucleating agent. Ind Eng Chem Res 50(21): 12299–12303

Ramiah MV (1970) Thermogravimetric and differential thermal analysis of cellulose, hemicellulose, and lignin. J Appl Polym Sci 14(5):1323–1337

Shafizadeh F, Bradbury AGW (1979) Thermal degradation of cellulose in air and nitrogen at low temperatures. J Appl Polym Sci 23(5):1431–1442

Shanks RA, Hodzic A et al (2006) Composites of poly(lactic acid) with flax fibers modified by interstitial polymerization. J Appl Polym Sci 99(5):2305–2313

Shibata M, Ozawa K et al (2003) Biocomposites made from short abaca fiber and biodegradable polyesters. Macromol Mater Eng 288(1):35–43

Tsujia H, Tezukaa Y et al (2005) Spherulite growth of L-lactide copolymers: effects of tacticity and comonomers. Polymer 46(13):4917–4927

Van de Velde K, Baetens E (2001) Thermal and mechanical properties of flax fibres as potential composite reinforcement. Macromol Mater Eng 286(6):342–349

Wang C, Liu C-R (1999) Transcrystallization of polypropylene composites: nucleating ability of fibres. Polymer 40(2): 289–298

Xiao HW, Li P et al (2010) Isothermal crystallization kinetics and crystal structure of poly(lactic acid): effect of triphenyl phosphate and talc. J Appl Polym Sci 118(6):3558–3569

Yuryev Y, Wood-Adams P et al (2008) Crystallization of polylactide films: an atomic force microscopy study of the effects of temperature and blending. Polymer 49(9): 2306–2320

Zafeiropoulos NE, Baillie CA et al (2001) A study of transcrystallinity and its effect on the interface in flax fibre reinforced composite materials. Compos A Appl Sci Manuf 32(3–4):525–543